



Experimental Modeling and Evaluation Sediment Scouring in Riverbeds around Downstream in Flip Buckets

K. Khalifehei^{*a}, G. Azizyan^a, M. Shafai-Bajestan^b, K. W. Chau^c

^a Department of Civil Engineering, University of Sistan and Baluchestan, Zahedan, Iran

^b Department of Hydraulic Structures, Faculty of Water Science Engineering, Shahid Chamran University of Ahvaz, Ahwaz, Iran

^c Department of Civil and Structural Engineering, Hong Kong Polytechnic University, Yuk Choi Road, Hung Hom, Kowloon, Hong Kong

PAPER INFO

Paper history:

Received 14 May 2020

Received in revised form 8 July 2020

Accepted 04 August 2020

Keywords:

Sediment Scour

Sediment Transport

Hydraulic Structures

Stilling Basin

Large Dam

ABSTRACT

Flip buckets are a common configuration for side channel spillways. Similar to other spillways, the flip bucket or ski jump has its disadvantages, among which the scour hole downstream due to the flip bucket jet is the most important. The structure safety and stability may be influenced by the scour holes generated at the downstream side of bucket type energy dissipators. This study has employed an experimental model in order to examine the sediment scour created at the end of flip bucket energy dissipators at various flow rates and tail water depths. A total of 45 experiments were performed under different conditions. The experimental investigation was conducted at the hydraulic laboratory of Shahid Chamran University in Iran. The main objective of this research was to identify the maximum depth of sediment scour (d_{sm}) and the maximum distance of sediment scour hole (L_{sm}) from the structures. The results showed that the maximum depth of scour and its distance from the structure increased by increasing discharge. The results of experimental models show that, at the downstream depths (Y_f) of 0.2 and 0.3 m, the stack was formed by the scouring at the upstream side of the hole, and at a depth of 0.1 m, this stack was transferred to the area after the scour hole. This could be explained by the fact that at downstream depths of 0.2 and 0.3 m, the rolling flow moved from the bottom upwards in the opposite direction of the water flow and sequestered the sediments upstream. According to Equation Mean Absolute Relative Error (MARE) proposed relation based on laboratory studies has MARE of about 34.2%.

doi: 10.5829/ije.2020.33.10a.09

1. INTRODUCTION

The erosion and morphological changes of the rivers naturally arise from the erosive effects of the water flow as well as the construction of various hydraulic structures in the waterway. Excessive erosion can gradually weaken the foundation of hydraulic structures and ultimately lead to their failure. The sediment scour at the downstream area of hydraulic structures represents a highly important zone for research because it is frequently occurring in engineering installations. In different countries around the world, various methods have been proposed for protection against scouring. These methods include rip-

rap, concrete block unit armor, articulated block mattress, gabions mattress, green coatings, stabilizers, etc. [1, 2].

Dams reservoirs not only suppress floods but also provide water for activities such as aquaculture human consumption, irrigation, industrial use and navigability. The release of stored water behind these structures produces a lot of energy at the downstream side and the bases of hydraulic structures. The kinetic energy that turbulent jets produce may lead to erosion at downstream channels and failure at hydrological constructions. It, therefore, entails local scour at the downstream regions of such hydraulic structures as vertical barrages, flip bucket jets, spillways and culverts. In general, the

*Corresponding Author: kamran.khalifehei@pgs.usb.ac.ir
(K. Khalifehei)

structures which dissipate energy are commonly utilized in order to prevent such issues. These protective structures dissipate the excessive energy that turbulent jets carry [3]. One of these dissipating structures is known as the flip bucket jet, which is designed as an attachment to the spillway that mixes the air and jet by conducting high velocity flows upwards and reduces the impact of the jet core and the flow of jets from the structure. The flip bucket jet is designed with various jet angles, radii and structures. This structure is an economical alternative to other conventional dissipators such as stilling basins, etc. [4, 5]. So far several studies have been carried out to address scouring downstream of flip bucket jets by Bormann and Julien [6]; Jafari and Khiavi [7], Mason and Arumugan [8], Amanian and Urroz [9], Stein et al. [10], Afify and Urroz [11] and Cordier et al. [12]. Furthermore, scholars such as Hoffmans and Verheij [13], Khalifehei et al. [14], Ghodsian et al. [15], Juon and Hager [16], Pagliara et al. [17], Yamini [18], and Movahedi et al. [19] used experimental data to provide empirical predictive relationships for the maximum depth of scour caused by the jet. The results of their studies were presented as non-dimensional diagrams and relations. Few quantitative studies were undertaken regarding the erosion pattern as well as the maximum distance of the scour hole from the structures [20]. More recently, Zhang et al. [21], and Movahedi et al. [22] established an expression to predict the sediment scour depth using Flow3D or Fluent, a computational fluid dynamics (CFD) software [23-27].

A variety of hydraulic parameters (such as flow depth, flow velocity, jet impact angle, and turbulence intensity on the basin), hydrological factors (such as flood frequency, discharge flood, and flood duration) and geological parameters (such as the type of bed materials, grain size distribution, and cohesive or non-cohesive sediment) make the mechanism of scouring extremely complicated. The evolution of scouring characteristics is one of the significant issues in hydraulic and hydrology engineering. Over the past five decades, numerous empirical formulations, based on the regression of the scouring data observed from laboratory experiments in the field, have been developed to predict scouring characteristics (typically the equilibrium scour depth); nevertheless, these empirical formulations are sensitive to the uncertainty of effective parameters and in some cases could not comprehend the actual internal mechanism between variables. The motivation of the current research is to exhibit all the established research works on the implementation of empirical formulations models for multiple scouring depths modeling such as ski jump, flip bucket, and spillway structures. A comprehensive review of the up-to-date research works on the scouring depth phenomena is presented, placing special emphasis on the recent and basic applications of empirical formulations models and also recalling all the

performed experimental laboratory studies. The review includes an informative evaluation and assessment of the surveyed research efforts. The improvement in prediction performance provided by the empirical formulations models when compared to empirical formulations is discussed. It should be noted that the process of scour at the downstream side of a ski jump is experimentally investigated using three different non-cohesive bed materials with the densimetric Froude number, the Reynolds Number of the jet, the angle of the ski jump lip, and the sediment non-uniformity constant taken into consideration. In the final section of this paper, the results and achievements of the experimental studies are briefly presented.

2. MATERIALS AND METHODS

2. 1. Empirical Formula for Calculating the Maximum Depth of Scour

The formulas developed for estimating sediment scour under a jet flow are collected in Table 1. The authors list them and, where the author has developed more than one expression, they are also referenced by a letter. These Equations can be generally written as:

$$d_s = \frac{cq^x H^y \alpha^w}{d^z} \quad (1)$$

In which d_s scour depth, in terms of the head drop from upstream to downstream water level H , the unit discharge of the jet at the point of impact q , angle of impact jet α , and, in some cases, the characteristic particle size of the bed material d . Also, other terms c , x , y , z and w are all constant for any given formula.

It may be noted, based on Table 1, that first the maximum sediment scour depth is considered a function of q (the discharge per width), H (at bucket lip level), or H_1 (at tailwater level) is the second to play a role [32]. The bed sediment materials diameter and the angle of impact of the jet flow (α) play no significant parts. Schoklitsch [25], Chee and Kung [28] noted that the particles diameter have a significant impact. Chee and Kung [28] used α angle in their formulas. Schoklitsch [25] used d_{90} (a sediment diameter bigger than 90% of materials) in his computations, whereas they took d_{50} into consideration [28].

2. 2. Dimensional Analysis

To determine the scouring pattern of the bed in a laboratory model under the changes in the size of bed sediments and to make a comparison with other existing relations, it is necessary first to carry out a precise dimensional analysis using the parameters affecting this phenomenon. The most important parameters affecting the scouring phenomenon, according to Figure 1, are stated as Equation (2):

TABLE 1. Literature empirical formula proposed for estimation of the maximum scour depth

Method	Equation	c	x	y	z	w
Schoklitsch [25]	$d_s = \frac{0.521q^{0.57}H^{0.2}}{d^{0.32}}$	0.521	0.57	0.2	0.32	0
Veronese I [26]	$d_s = \frac{0.202q^{0.54}H^{0.225}}{d^{0.42}}$	0.202	0.54	0.225	0.42	0
Veronese II [26]	$d_s = 1.9q^{0.54}H^{0.225}$	1.9	0.54	0.225	0	0
Damle I [27]	$d_s = 0.652q^{0.5}H^{0.5}$	0.652	0.5	0.5	0	0
Damle II [27]	$d_s = 0.543q^{0.5}H^{0.5}$	0.543	0.5	0.5	0	0
Damle III [27]	$d_s = 0.362q^{0.5}H^{0.5}$	0.362	0.5	0.5	0	0
Chee and Kung [28]	$d_s = \frac{1.663q^{0.6}H^{0.2}d^{0.1}}{d^{0.1}}$	1.663	0.6	0.2	0.1	0.1
Chee and Padiyar [29]	$d_s = \frac{2.126q^{0.51}H^{0.18}}{d^{0.061}}$	2.126	0.67	0.18	0.063	0
Wu [30]	$d_s = \frac{1.18q^{0.51}H^{0.6}}{d^{0.1}}$	1.18	0.51	0.6	0.1	0
Martins [31]	$d_s = 1.5q^{0.6}H^{0.6}$	1.5	0.6	0.1	0	0
Incyth [32] ()	$d_s = 1.413q^{0.5}H^{0.25}$	1.413	0.5	0.25	0	0
Khatsuria [20]*	$d_s = 0.9q^{0.5}H^{0.5}$	0.9	0.5	0.5	0	0
Azmathullah et al. [33]**	$d_s = 1.42q^{0.44}H_1^{0.3}$	1.42	0.44	0.3	0	0

Damle’s equation modified for the ultimate scour according to further data obtained from the laboratory and the field, proposed by Khatsuria [20]; ** H_1 : The head amid the upper water level and the tail water level (m).

$$d_s = f(V_t, Y_j, \theta, g, \vartheta, Y_{tsm}, d_{50}, D', \rho_w, \rho_s, \mu, T, t, \delta) \quad (2)$$

Some of the parameters of Equation (2) are presented in the previous sections, but the other parameters include d_s : the depth of the scour hole, Y_j : the mean flow depth at the lip of the ski jump, θ : the lip angle of the ski jump, ϑ : the jet impact angle on the basin, d_{50} : 50% finer particle sizes of sediment, D' : representative particle size, ρ_s : the sediment density, ρ_w : the water density, μ : the water dynamics viscosity, T : the turbulence intensity on the basin, t : time, δ : the geometric standard deviation of the sediment bed material size, and g : acceleration due to gravity. Taking into consideration that jet velocity at the lip of the ski jump (V_t), mean flow depth at the lip of the ski jump (Y_j) and density (ρ_w) are the repeating variables, the dimensionless grouping of Equation (3) is obtained:

$$\frac{d_s}{d_{50}} = f(Re, We, Fr, \frac{d_s}{d}, (\frac{\rho_s - \rho_w}{\rho_w}), D', T, \theta, \vartheta, \tau) \quad (3)$$

In this equation; $Fr = \frac{V_t}{\sqrt{gd}}$: the Froude number, $(\frac{\rho_s - \rho_w}{\rho_w})$: the relative specific density, $Re = \frac{\rho V_t Y_j}{\mu}$: the Reynolds number, $We = \frac{V_t}{\sqrt{\delta/\rho_w Y_j}}$: the Weber number, and $\tau = \frac{V_t t}{Y_j}$: the dimensionless time factor. The mean velocity of the flow may be written in a non-dimensional

form, as is usual in the research on the sediment scour produced under the action of free jets, as $F_g = \frac{V_t}{\sqrt{(\frac{\rho_s - \rho_w}{\rho_w})gd_{50}}}$; where V_t denotes the velocity of the jet at the ski jump jet, $(\frac{\rho_s - \rho_w}{\rho_w})$ is the relative sediment density, ρ_s represents the sediment particle density, ρ_w is the water density, g is acceleration of gravity, and d_{50} denotes the sediment material particle size.

2. 3. Equipment and Testing Methods The experiments were carried out in a flume with a length, width and depth of 7.3, 0.65 and 0.6 m, respectively, and a longitudinal slope of 0.0028 at the hydraulic experimental laboratory of Shahid Chamran University in Iran. At upstream of the flume, an ogee spillway connects the reservoir to a galvanized flip bucket with a radius of 0.16 m through a chute. This work incorporated bed materials whose δ (geometric standard deviation) values refer to their non-uniform nature. The investigated bed material was a uniformly sanded gravel with a grain size distribution of $D_{50} = 2.31 \text{ mm}$. Bed materials were selected in a way to keep the value of about $D_{85} = 3.25 \times 10^{-3} \text{ m}$, $D_{90} = 3.64 \times 10^{-3} \text{ m}$, $\rho_s = 2.70 \text{ kg/m}^3$ and $D' = 1.78$. The walls and the bottom of the flume were made of transparent Plexiglas. The required flow entered the stilling tank from the water supply tank via a centrifuge pump at the beginning of the flume. With the

aim of eliminating the input turbulence, a distilling lattice plate was used at a distance of 1 meter from the flume inlet. The flow entered a pond after leaving the flume and then re-entered the water supply tank. The flow discharge was measured using an ultrasonic flow meter mounted on the inlet pipe of the pump. Due to the sub-criticality of the flow, the flow depth control was carried out using a sliding gate located at the end of the flume.

Point gauges with a precision of 0.2 millimeters were installed on a rail and helped measure levels of free surface, depths of flow, and depths of scouring. The flow rate has been measured with a 2.5% uncertainty. Measurements of the flow depth in the ski-jump helped calculations of the flow velocity of the jet.

The experiments were carried out at different discharges (q) between 0.005 and 0.03 (m^3/s) at different depths (Y_t) of 0.1, 0.2, and 0.3 m. It is worth noting that at high flows, the depth of the cavity reached the bottom of the flume due to the increase in scouring; therefore, this issue was not considered in the analysis of the experiments.

In the experiments, the distance between the sediment level and the edge of the jet was selected as $Y_{level} = 0.2 \text{ m}$. In this way, the depth of 0.1 m did not submerge the edge of the bucket. In the second case (0.2 m), the tail water depth was at the edge of the jet, and in the third case ($Y_t = 0.3 \text{ cm}$), the bucket was submerged (Table 2).

The scouring downstream of the flip bucket jet is a time function and increases over time until an equilibrium condition is reached. Hence, it is important for designers to identify the time needed for the hole to reach equilibrium. With the purpose of determining the equilibrium time of the tests, a 5-hour test was performed at a rate of 0.025 (m^3/s) and the equilibrium time, approximately 3 hours in this test, was obtained based on the slight changes in the scour hole versus time.

TABLE 2. Laboratory experimental conditions.

	Run 1	Run 2	Run 3	Run 4	Run 5
q (m^3/s)	0.005	0.01	0.015	0.02	0.025
	0.1	0.1	0.1	0.1	0.1
Y_t (m)	0.2	0.2	0.2	0.2	0.2
	0.3	0.3	0.3	0.3	0.3
Y_{level} (m)	0.2	0.2	0.2	0.2	0.2
Re	1.02×10^5	1.14×10^5	1.22×10^5	1.25×10^5	1.27×10^5
We^*	39	42	48	62	77

* Chanson et al. [34] suggested that in order to minimize the scale effects in a two-phased air water flow in a turbulent flow such as a jet, it is required that the Weber number and the Reynolds number be greater than $Re = 10^5$ and $We = 32$, respectively, which has been controlled and verified in these experiments.

At the beginning of each test, the slider was completely closed, and the water entered the flume slowly so that the water gradually entered the flume through a 0.102 m tube to allow the water to reach the desired level. The inlet gate was then opened to the flume tank, and the discharge into the reservoir was adjusted by reading the flow meter. As soon as the concurrent flow spilled, the end gate was opened to the point that the downstream water level remained constant. After the flow was completed for 3 hours, the end gate was closed, and the pump was switched off to allow the water in the channel to slowly drain from the bottom of the flume with no effects on the topography of the bed. After a few hours and full discharge of water from the channel, the topography of the bed was taken around the base in a 1×1 grid by the laser depth meter. The most important components of the laboratory model are the reservoir, the centrifuge pump, the input flow, the bottom transform, the flip bucket jet, the sedimentary bed and the sliding gate. Figure 1(a) shows the experimental system, and Figure 1(b) shows a schematic view of the section of the laboratory model and its important hydraulic and geometric parameters.

To guarantee replication of the prototype tests by these experiments, geometric and Froudian protocols of scaling were run in the models. The Froude law was incorporated in the present study because gravitational and inertial forces fundamentally affect the mobility of water in any ski-jump no matter in a spill way or in a bottom outlet design. Viscosity and surface tension must be modeled to allow accurate simulation of the two-phased flow (water and air). This refers to the Froude, Reynolds and Weber laws fulfillment at the same time. Theingi et al. [35] concluded that employing very small scale models might influence the scour dimensions despite the limited advice given to modellers. The scour profile data must be normalized to provide for a comparison between varied experimental scales, and after a dimensional analysis of the governing quantities, it has been customary to non-dimensionalize the scour depth and the scour length by respectively employing the maximum scour depth, d_{sm} , and the maximum scour length, L_{sm} [36]. This results in demonstration of an appropriate match between the classical profiles including those of Lim and Chin [37], Aminoroaya et al. [1, 23] and others. Nonetheless, incorporating d_{sm} and L_{sm} entails restriction of data to intersect the origin, which is the point of the maximum scour and the maximum scour length, potentially hiding any differences between the tests and the role that small scale models could play. In another dimensionless group with the scour depth and length normalized utilizing the tail water depth Y_t could be taken into consideration, and this may potentially prove more useful if the results are scaled to prototype dimensions. This analysis will employ the latter.

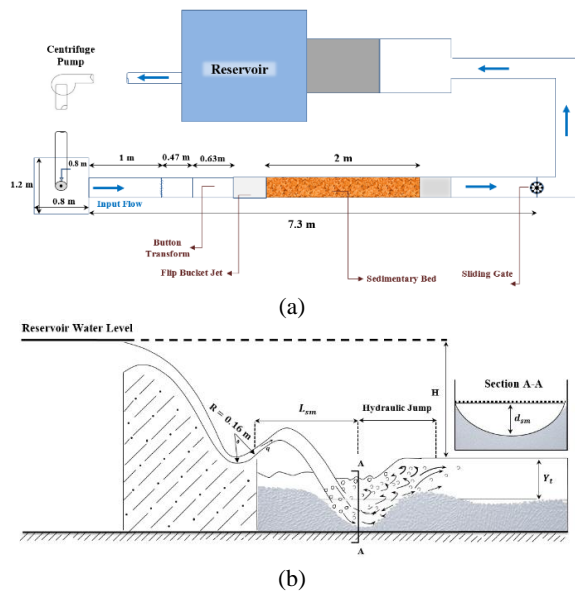
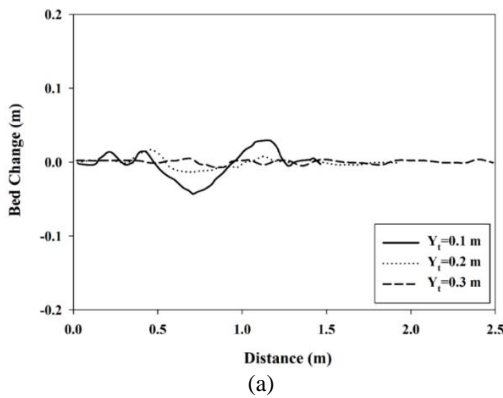
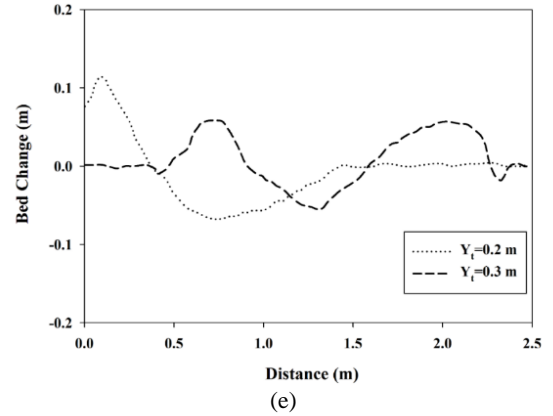
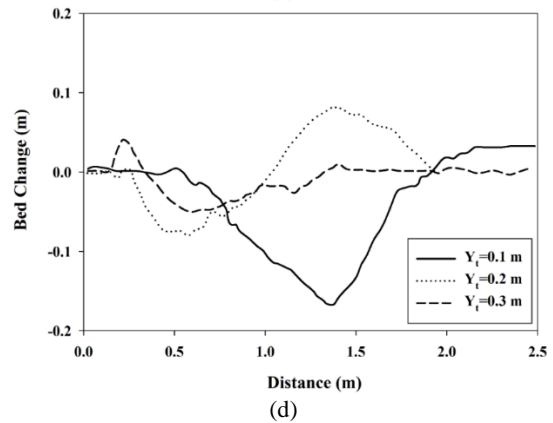
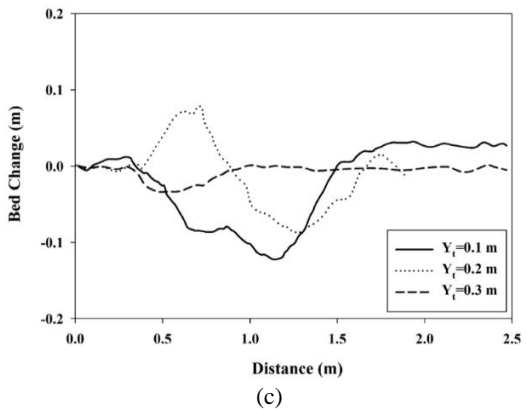
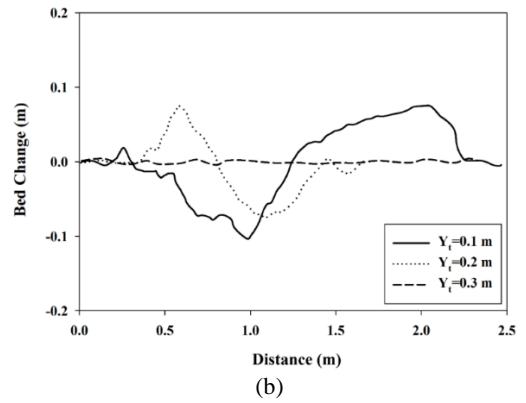


Figure 1. (a): Plan view of the experimental setup, and (b): Sketch of the experimental setup. Bucket radius (R), distance of the maximum scour from bucket lip (L_{sm}), total head (H), the maximum depth of scour (d_{sm}), tail water depth (Y_t), discharge intensity (q), bucket lip angle (θ). Section A-A configuration of geometric parameters of d_{sm} and Cross section of scour

3. RESULTS AND DISCUSSION

3.1. Analysis of the Scouring Pattern In Figure 2, the longitudinal profile of the bed is shown at the downstream side of the flip bucket under different flows conditions. According to Figure 2, the water pad prevents erosion and reduces scouring by increasing depth. The overall profile of different flows shows that when the flow increases, especially at lower depths, a larger length is affected by erosion and sedimentation. It also decreases as the depth increases.



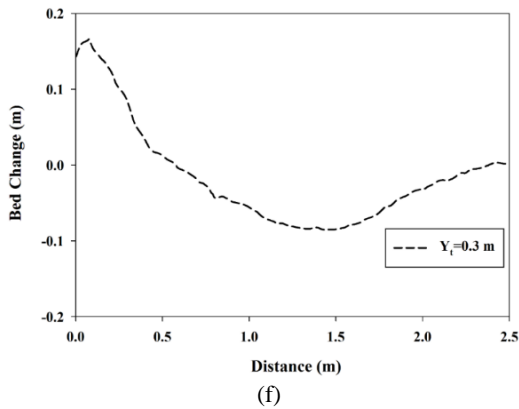


Figure 2. Variations in the longitudinal profile of the bed at different downstream depths of (a) 5 lit/s, (b) 10 lit/s, (c) 15 lit/s, (d) 20 lit/s, (e) 25 lit/s, and (f) 30 lit/s

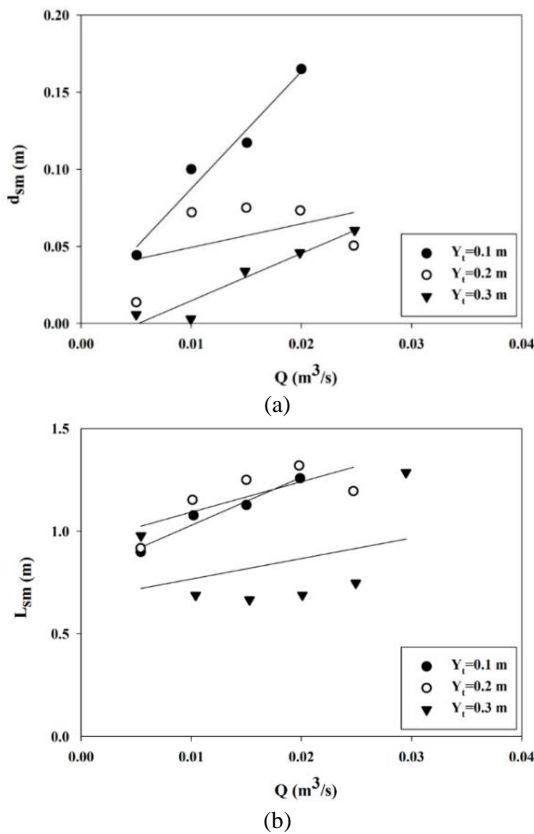


Figure 3. Variations in: (a) the maximum depth of the scour hole; and (b) the distance of the maximum scour from bucket lip (L_{sm}) at different flow rates

Figures 3(a) and 3(b) present the longitudinal profile of the bed for different discharges and tail water depths. As shown in Figure 3(a), increasing the depth of tail water (Y_t) will reduce the depth of scour (d_{sm}). Also, Figure 3(b) shows that increasing the flow discharge (Q) will increase the distance of the maximum scour from bucket lip (L_{sm}). Increasing the flow discharge (Q) will

increase the jet velocity and cause the jet to hit the bed farther away.

Moreover, at the downstream depths (Y_t) of 0.2 and 0.3 m, the stack was formed by the scouring upstream of the hole, and at a depth of 0.1 m, this stack was transferred to the area after the scour hole. This could be explained by the fact that at downstream depths of 0.2 and 0.3 m, the rolling flow moved from the bottom upwards in the opposite direction of the water flow and sequestered the sediments upstream. By reducing the depth to 0.1 m, the rolling flow containing suspended sediments was transmitted downstream by the inlet jet due to the high flow rate, and the sequestration occurred at the bottom of the hole by reducing the speed of the inlet jet.

Variations in the normalized scour depth d_{sm}/Y_t with the densimetric particle Froude number (F_g) are shown in Figure 4(a). The results showed that as the densimetric particle Froude number increased and the depth declined, the water pad had a low ability under the jet's dynamic force, and the amount of erosion rose. Besides, L_{sm}/Y_t variations versus the Froude number of the particle (F_g) are shown in Figure 4(b). According to the figure, the distance of the maximum scour from bucket lip expands with the increase in the Froude number.

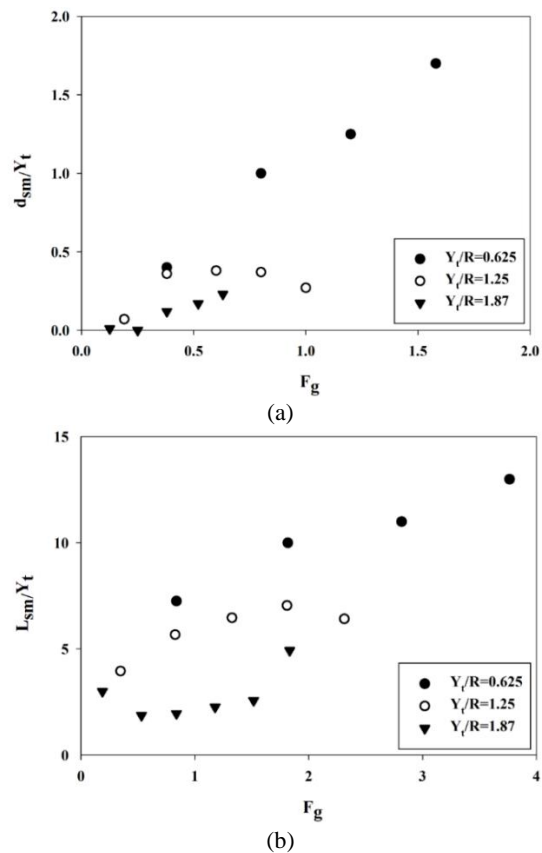


Figure 4. Variations in (a) d_{sm}/Y_t ; and (b) relative to the particle's Froude number

In this study, the above-mentioned dimensionless groups of parameters were related to each other based on non-linear regression (SPSS 22 software). This yielded the following equations for estimating the maximum depth of scour, the maximum scour width, and the distance of the maximum scour location, respectively. This relation is derived to predict the maximum scour depth and the distance of the maximum scour from bucket lip (L_{sm}), and to compare the results with previous investigations (Equations (4) and (5)):

$$\frac{d_{sm}}{Y_t} = 0.12(F_g)^{0.8} \left(\frac{H}{Y_t}\right)^{1.12} \tag{4}$$

$$\frac{L_{sm}}{Y_t} = 2.7(F_g)^{0.37} \left(\frac{H}{Y_t}\right)^{0.69} \tag{5}$$

Figures 5(a) and 5(b) present the experimental and calculated normalized scour depths d_{sm}/Y_t derived using Equations (4) and (5) relative to the 45° line. A comparison of the results showed that despite the complexity of the scouring phenomenon, the relations had good accuracy for predicting these parameters in the flip bucket jet structure. The coefficient of determination R^2 and the minimum root-mean-square error (RMSE) were 0.97 and 0.8, respectively, for Equation (4), while these values were 0.94 and 0.8 for Equation (5), respectively.

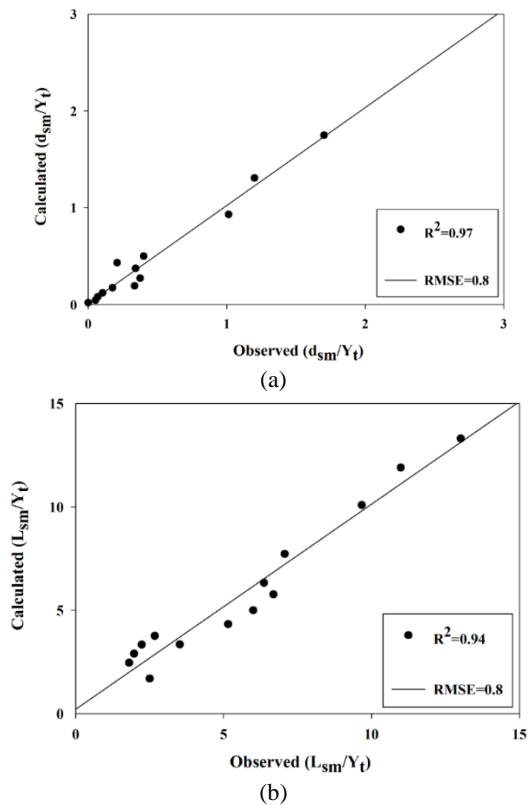


Figure 5. A comparison of experimental and regression model results (a) Equation (4), and (b) Equation (5)

In Figure 6(a), the linear regression fit was made between the experimental values and the calculated values presented for the dimensionless parameter $\frac{d_{sm}}{Y_t}$ (Equation (4)), so that the correlation coefficient R^2 and the regression line slope α equaled 0.97 and 1.01, respectively, which suggested a very good performance of the relationship. Moreover, in Figure 6(b), the same comparison was made for Equation (5), so that the correlation coefficient R^2 and regression line slope α equaled 0.93 and 0.98, respectively, which also showed that the relationship had a good performance.

To evaluate the presented relations (Table 2), the results of this study were compared with the relationships provided by other studies in Figure 7. Azmathullah et al. [33] proposed the equations below for the evaluation of the maximum depth of scour and the distance between the hole and the structure (Equations (6) and (7)):

$$\frac{d_s}{Y_t} = 6.914 \left(\frac{q}{\sqrt{gY_t^3}}\right)^{0.694} \left(\frac{H}{Y_t}\right)^{0.0815} \left(\frac{R}{Y_t}\right)^{-0.233} \left(\frac{d_{50}}{Y_t}\right)^{0.196} \theta^{0.196} \tag{6}$$

$$\frac{d_s}{Y_t} = 9.85 \left(\frac{q}{\sqrt{gY_t^3}}\right)^{0.42} \left(\frac{H}{Y_t}\right)^{0.28} \left(\frac{R}{Y_t}\right)^{0.043} \left(\frac{d_{50}}{Y_t}\right)^{0.037} \theta^{0.346} \tag{7}$$

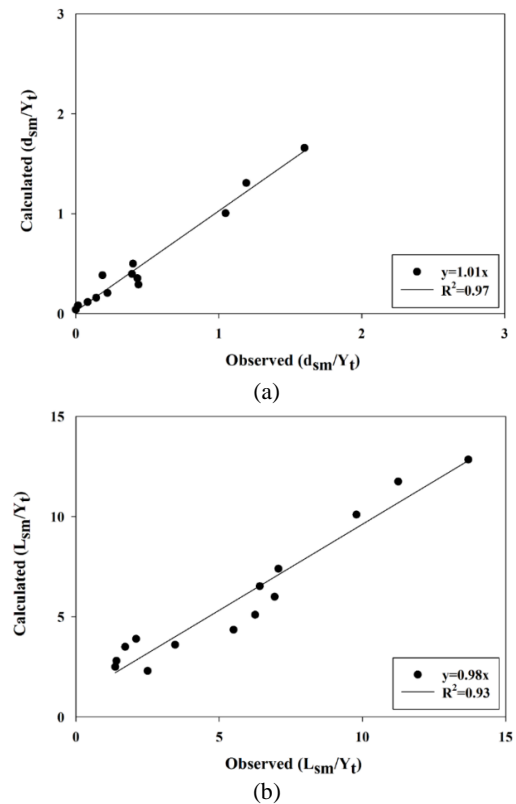


Figure 6. Regression fit of experimental and calculated results (a): Relative scour depth (d_{sm}/Y_t), and (b): Relative distance of the maximum scour from bucket lip (L_{sm}/Y_t)

where H represents the head between the upper (reservoir) water level and the tailwater level, and R is the radius of the bucket. Besides, Naghikhani et al. [38] suggested similar relationships for estimating the scour hole depth and its distance from the structure using the granular computing method as Equations (8) and (9):

$$\frac{d_s}{Y_t} = 1.94 + 0.389 \left(\frac{q}{\sqrt{gY_t^3}} \right) - 19.414 \left(\frac{d_{50}}{Y_t} \right) - 0.504 \left(\frac{R}{Y_t} \right) \quad (8)$$

$$\frac{d_s}{Y_t} = 3.117 + 0.21 \left(\frac{q}{\sqrt{gY_t^3}} \right) + 0.904 \left(\frac{H}{Y_t} \right) \quad (9)$$

Figure 8 shows the comparison of the experimental results with previous studies, including those of Mason [39], Sofrelec [40], Jaeger [41], and Yen [42]. As shown in Figure 8, the proposed relationship of the present study is in very good agreement with previous relationships. Also, the regression coefficient (R^2) of the proposed relationship is higher than previous relationships and increases the accuracy of predicting the depth of scour.

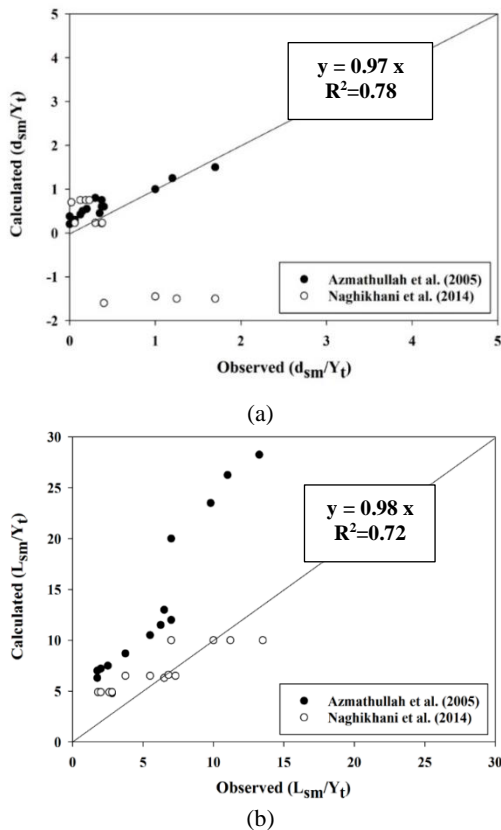


Figure 7. A comparison of experimental results with equations provided by previous researchers (a): scour depth, and (b): distance of the maximum scour from bucket lip (the reason for the significant differences is the different experiment conditions of Azmathullah et al. [33] and Naghikhani et al. [38])

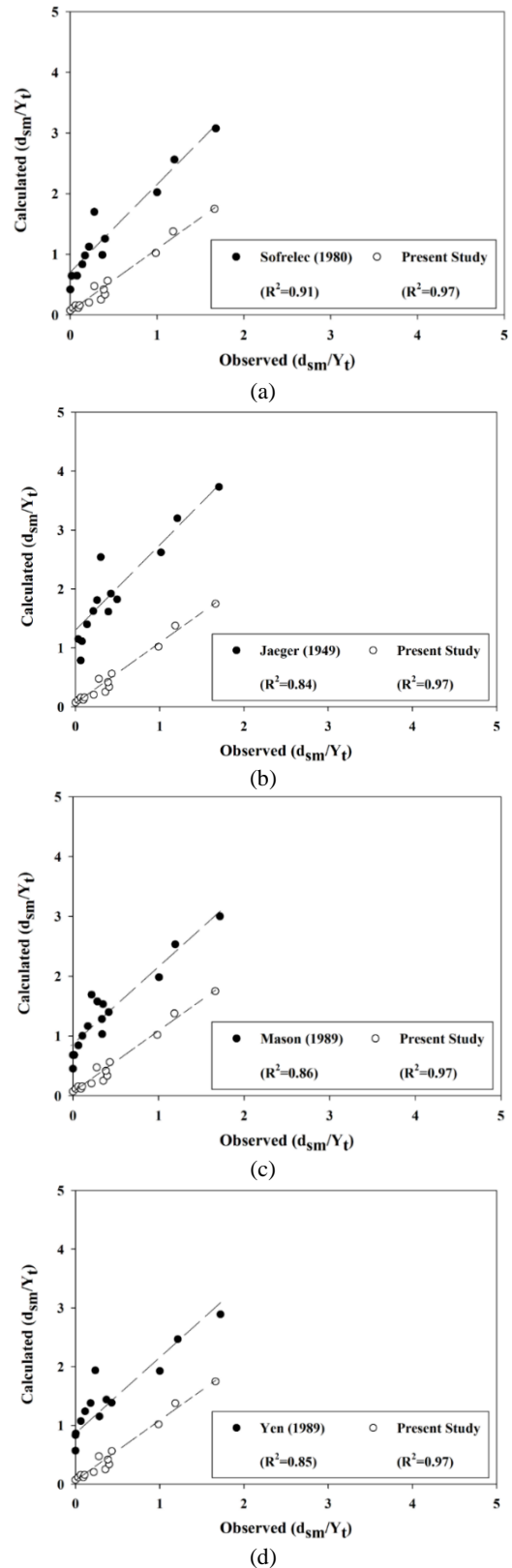


Figure 8. A comparison of experimental and calculated values of the dimensionless parameter d_{sm}/Y_t in previous studies; (a) Sofrelec [40], (b) Jaeger [41], (c) Mason [39], and (d) Yen [42]

3. 2. Comparison and Analysis of Empirical Formulas for Scour Depth

Because the most important parameters of scouring are q , H , Y_t and the bed materials size (d_{50}) for d_{sm} estimation, the generalized form can be shown as Equation (10):

$$d_{sm}/Y_t = k \frac{q^\alpha H^\beta}{Y_t d_{50}^\gamma} \tag{10}$$

where k (an experimental value) is a multiplication constant, while α , β , and γ are exponential constants. Table 3 provides a list of these constants matching various scour depth estimation formulas. It is noteworthy that the values of k fall into a wide range between 0.36 and 3.27, while α values vary over a much shorter range of 0.45 and 0.7; β between 0.05 and 0.5; and γ between 0.062 and 0.32, which means k variation can result in a wide range of values for ds with different formulas applied (Table 3) [38-44].

Table 3 presents the formula which were employed to predict d_{sm} matching different experimental data including q , H , d_{50} , and Y_2 as reported in previous studies. Then, as also illustrated in Figures 9 and 10, the d_{sm} calculated through this list was compared to the empirical ds . There is a linear relationship between the estimated depth obtained from experimental formulas and the scour depth collected in the laboratory, as shown in Equation (11).

$$\text{Estimated depth with empirical formulae } (d_{sm}) = (\Gamma) \times \text{observed depth in the experiment } (d_{sm}) \tag{11}$$

As shown by the constant Γ values provided in Table 4, the experimental formulas accurately predict the scour depth. Table 4 presents a summary of such values with the aim of estimating the scour depth according to experimental data.

When Γ approaches unity, the estimation is considered accurate. If such a value is smaller or greater than 1, underestimation and overestimation occur respectively. These figures along with Table 4 refer to the fact that none of the equations produced a perfect prediction for d_{sm} with the exception of Federspiel [47]. Equations such as Schoklitsch [25], and Hartung [43] exhibited over prediction of d_{sm} ; whereas, equations such as Martins [31], Mason [39], Ervine et al. [44] and Castillo [45] underpredicted d_{sm} . With a more careful investigation into the results, it is concluded that most overestimated equations produce great values ($k > 1.5$). For $k < 1$, the values are mostly underpredicted. For Federspiel [47] and Fiorotto et al. [49] formulas, $1 < k < 1.5$, d_{sm} prediction is better than other relations. It can be further noted that there is not much influence of exponential parameters of Equation (9) [38-44].

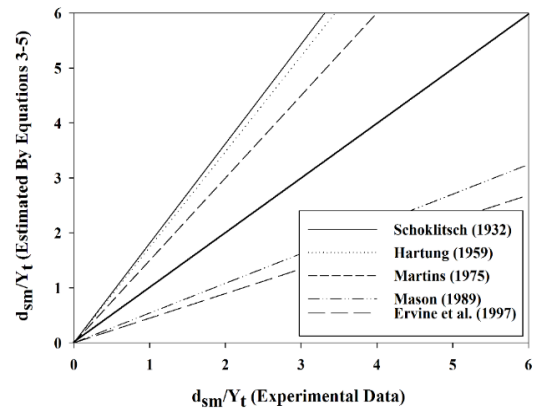


Figure 9. Estimates with empirical formula and the observed sediment scour depth according to laboratory data using Equations (1) to (5) listed in Table 3

TABLE 3. Coefficients for sediment scour prediction formulas

No. of Eq.	Author (Year)	k	α	β	γ
1	Schoklitsch [25]	0.52	0.57	0.20	0.32
2	Hartung [43]	1.4	0.64	0.36	0
3	Martins [31]	1.5	0.6	0.42	0.1
4	Mason [39]	3.27	0.6	0.05	0.3
5	Ervine et al. [44]	0.36	0.55	0.5	0
6	Castillo [45]	2.2	0.65	0.2	0.06
7	Melo et al. [46]	1.67	0.7	0.2	0.1
8	Federspiel [47]	1.5	0.6	0.1	0
9	Castillo and Carrillo [48]	0.63	0.45	0.25	0.12
10	Fiorotto et al.[49]	2.3	0.6	0.1	0.24

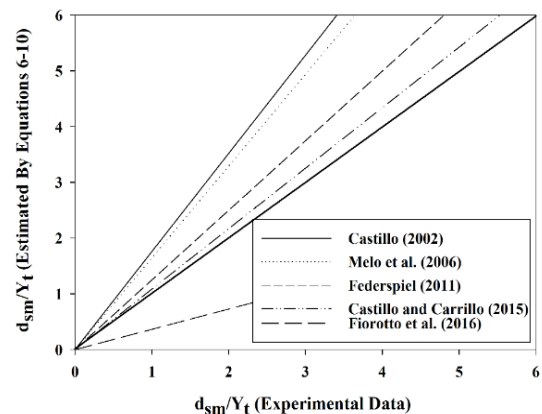


Figure 10. Estimates with empirical formula and the observed sediment scour depth according to laboratory data using Equations (5) to (10) in Table 3.

TABLE 4. Summary of Γ values for sediment scour depth prediction according to experimental data

No. of Eq.	Author (Year)	Γ	Remark
1	Schoklitsch [25]	1.78	overprediction
2	Hartung [43]	1.43	overprediction
3	Martins [31]	0.56	underprediction
4	Mason [39]	0.48	underprediction
5	Ervine et al. [44]	0.32	underprediction
6	Castillo [45]	1.75	overprediction
7	Melo [46]	1.82	overprediction
8	Federspiel et al. [47]	1.10	Best prediction
9	Castillo and Carrillo [48]	0.38	underprediction
10	Fiorotto et al. [49]	1.3	overprediction

3. 3. Evaluation of the Effect of Particle Size on Ski Jump Scour

To be more comprehensively stated, it is anticipated that an increase in the velocity of the jet flow and the density of fluid increases the depth of the sediment scour hole. To the contrary, it is expected that addition of density and size of the particle distribution materials decreases the scour depth. Experiments carried out on prototypes demonstrated that air entrainment into the fluid reduces the scour depth under the same flow conditions [45]. There is a simple physical interpretation of these phenomena. The specific weight of the aerated flow is less than that of the non-aerated flow. Mason and Arumugam [8] showed that the angle of jet impinging on the stilling basin is a function of the bucket lip angle (θ) and jet velocity (V_j) and thus, the parameter (ϑ) can be removed from the dimensional analysis list (Equation (3)). Due to the fact that the analysis on the results of scour depth values was performed under the scour hole equilibrium, the time parameter (t') is also removed from the dimensional analysis. According to Chanson [34] and Pagliara et al. [17] studies, the jet flow leaving the ski jump will be a fully developed flow (Tu : Turbulence intensity) controlled by the Reynolds and Froude numbers, and this parameter can be removed from the dimensional analysis. Yamini et al. [50, 51] and Chanson et al. [34] suggested that in order to minimize the scale effects in a two-phased air water flow in a turbulent flow such as a jet, it is required that the Weber number and Reynolds number be greater than $Re = 10^5$ and $We = 32$, respectively, which has been controlled and verified in these experiments (Table 2). Accordingly, Equation (12) can be summarized as follows:

$$\frac{d_s}{d_{50}} = f(Re, F_g, \theta, D') \tag{12}$$

By using the experimental model, attempts have been made to confirm Equation (12) using the changes in bed material. Thus, according to Table 5, the specifications of

bed materials are evaluated in the laboratory model in the following three cases. With the aim of confirming the assumptions given in Equation (12), the relative depth of scouring versus the variation of the squared densimetric particle Froude number (F_g^2) are plotted based on the experimental model results. The dependence between the parameters of relative depth variations and the densimetric particle Froude number is evident in Figure 11.

By performing multivariate regression on different experimental conditions using the Sigmaplot software, the following equation is obtained with the regression coefficient $R^2 = 0.89$, which is presented in Equation (13):

$$\frac{d_s}{d_{50}} = \frac{0.08 \cdot (Re)^{0.227} \cdot (F_g^2) \cdot \sin\theta}{D'} \tag{13}$$

For comparison of the present relation with other relations in this context, it should be noted that in most relations, not all parameters of dimensional analysis are involved in the relations. Accordingly, the multivariate regression was repeated using the experimental model data, and due to the smaller effect, the parameters of bucket lip angle and sediment density are not involved in this relation. Figure 12 is presented to compare the experimental data with other previous studies. This diagram is based on the data from individuals such as

TABLE 5. Type of the sand materials employed in the experimental investigation

Type of Sand (1)	Type of Sand (2)	Type of Sand (3)
$D_{50} = 2.31 \times 10^{-3} \text{ m}$	$D_{50} = 5.42 \times 10^{-3} \text{ m}$	$D_{50} = 7.57 \times 10^{-3} \text{ m}$
$D_{85} = 3.25 \times 10^{-3} \text{ m}$	$D_{85} = 6.83 \times 10^{-3} \text{ m}$	$D_{85} = 8.87 \times 10^{-3} \text{ m}$
$D_{90} = 3.64 \times 10^{-3} \text{ m}$	$D_{90} = 7.23 \times 10^{-3} \text{ m}$	$D_{90} = 9.24 \times 10^{-3} \text{ m}$
$\rho_s = 2.70 \text{ kg/m}^3$	$\rho_s = 2.70 \text{ kg/m}^3$	$\rho_s = 2.70 \text{ kg/m}^3$
$D' = 1.78$	$D' = 1.32$	$D' = 1.19$

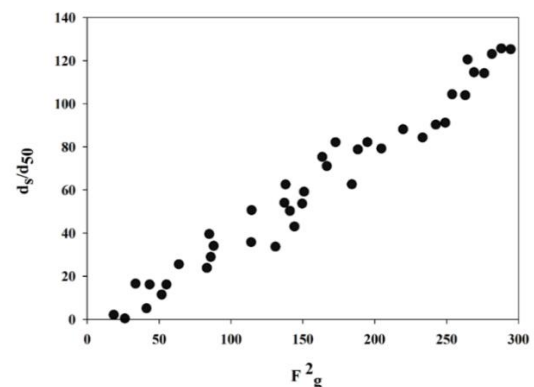


Figure 11. Normalized scour depths vs. F_g^2

Azmathullah et al. [33], Movahedi et al. [22], Amanian and Urroz [9], and Castillo and Carrillo [48]. Accordingly, the simpler regression relation is presented as Equation (14):

$$\frac{d_s}{d_{50}} = 0.23 \cdot (Re)^{0.048} \cdot (F_g^2) \tag{14}$$

In this case, the regression coefficient is $R^2 = 0.92$, which is a relatively high coefficient. In order to compare the relation presented in this study with relations provided by other researchers for estimating the scour values due to the jet impingement on the bed of the stilling basin, the mean relative absolute error is considered based on Equation (15):

$$MARE = \frac{1}{n} \sum_{i=1}^n \left(\frac{|(d_s)_{calculated} - (d_s)_{empirical}|}{(d_s)_{calculated}} \right) \tag{15}$$

According to Equation (15), parameters (n) are the numbers of laboratory observations and the parameters $(d_s)_{calculated}$, and $(d_s)_{empirical}$ are the computational and measurement values of the scour depth, respectively. The proposed relation based on laboratory studies has MARE of about 34.2%, while the studies by Azmathullah et al. [33] and Amanian and Urroz [9] have an error of 38.2% and 72.9%, respectively. It should be noted that the present relations have two input variables, while their relations have four input variables. Other relations presented in the table have a relative absolute error of more than 100%. Using the relation presented in the range of Reynolds and Weber numbers, acceptable results can be predicted for the bed sediments over a relatively large range (see Figure 13).

The proposed relation based on laboratory studies has MARE of about 34.2%, while the studies by Azmathullah et al. [33] and Amanian and Urroz [9] have an error of 38.2% and 72.9%, respectively.

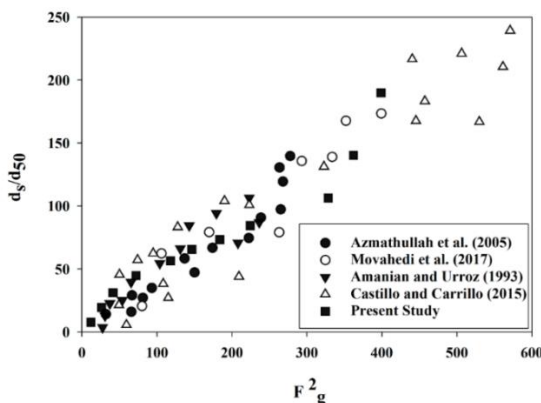


Figure 12. The depth of scour ($\frac{d_s}{d_{50}}$) normalized as a function of (F_g^2) with different Reynolds numbers (Re). Source: Azmathullah et al. [33], Movahedi et al. [22], Amanian and Urroz [9], Castillo and Carrillo [48], and the present work

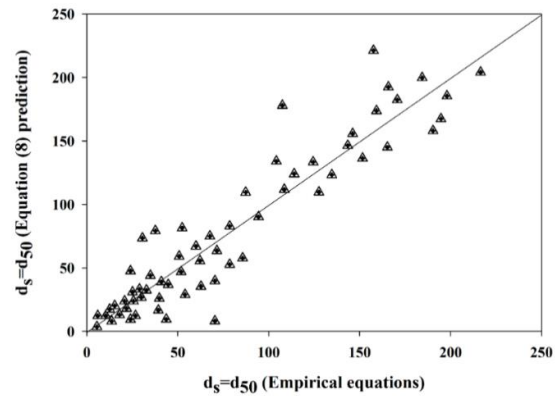


Figure 13. Equation (14) estimation of capacity by applying the data measurements obtained from the present work, Azmathullah et al. [33], Movahedi et al. [22], Amanian and Urroz [9], and Castillo and Carrillo [48], and comparing it with the line of 100% agreement

4. CONCLUSION

The main purpose of this study is to exhibit all the established research works on the implementation of empirical formulations models for multiple scouring depths modeling such as ski jump, flip bucket, and spillway structures. It presents an extensive review on the state of the art research studies on the scour depth phenomena with a specific focus on the most recent and basic implementation of models of experimental formulas as well as references to every experimental laboratory study carried out.

The results of experimental models show that, at the downstream depths (Y_t) of 0.2 and 0.3 m, the stack was formed by the scouring upstream of the hole, and at a depth of 0.1 m, this stack was transferred to the area after the scour hole. This could be explained by the fact that at downstream depths of 0.2 and 0.3 m, the rolling flow moved from the bottom upwards in the opposite direction of the water flow and sequestered the sediments upstream. By reducing the depth to 0.1 m, the rolling flow containing suspended sediments was transmitted downstream by the inlet jet due to the high flow rate, and the sequestration occurred at the bottom of the hole by reducing the speed of the inlet jet.

According to Equation $MARE = \frac{1}{n} \sum_{i=1}^n \left(\frac{|(d_s)_{calculated} - (d_s)_{empirical}|}{(d_s)_{calculated}} \right)$, parameters n are the numbers of laboratory observations and the parameters $(d_s)_{calculated}$, and $(d_s)_{empirical}$ are the computational and measurement values of the scour depth, respectively.

Most of the energy distributed by the flip buckets system is found at the impact point of the jet and the tail water and riverbed. Such an impact means enough force, which changes the riverbed topography even in spite of hard rock materials included in the bed. Hence, implementation of flip buckets must only be advised in

case the bed scour, because of the impacting jet, does not have an adverse influence on the dam and other structures such as the flip bucket, or has no harms to the environment. The equation presented in the study is different from the existing empirical equations since it also involves (Fr^2) , which physically means that Fr_d^2 has a direct relationship with hydrodynamic forces leading to scour; whereas, it has an indirect relationship with scour-resistant forces. Therefore, the conclusion is that the scour process is under the influence of the force on the bed materials entrained in the jet flow. This force is related to the velocity squared but is reversely related to the density on a linear basis. Thus, this approach physically justifies the sediment scour process in 3 phases of “water, air, and soil”.

5. REFERENCES

- Aminoroayaie Yamini, O., S. Hooman Mousavi, M. R. Kavianpour, and Azin Movahedi. “Numerical Modeling of Sediment Scouring Phenomenon around the Offshore Wind Turbine Pile in Marine Environment.” *Environmental Earth Sciences* Vol. 77, No. 23, (2018), 776-787, Doi: 10.1007/s12665-018-7967-4.
- Ekeleme, Anthony Chibuzo, and Jonah C. Agunwamba. “Experimental Determination of Dispersion Coefficient in Soil.” *Emerging Science Journal*, Vol.2, No. 4, (2018), 213-218.
- Ghorbani, Mortaza Ali, Majid Pasbani Khiavi, and Parya Ahmadi. “Investigation of Nonlinear Behavior of Concrete on Seismic Performance of an Arch Dam Using Finite Element Method.” *Civil Engineering Journal*, Vol 2, No. 6, (2016), 295-305. doi:10.28991/cej-2016-00000034.
- Emeka, Arinze Emmanuel, Agunwamba Jonah Chukwuemeka, and Mama Benjamin Okwudili. “Deformation Behaviour of Erodible Soil Stabilized with Cement and Quarry Dust.” *Emerging Science Journal*, Vol 2, No. 6, (2018), 383. Doi: 10.28991/esj-2018-01157
- Ghodsi, Habibeh, and Ali Asghar Beheshti. "Evaluation of Harmony Search Optimization to Predict Local Scour Depth around Complex Bridge Piers." *Civil Engineering Journal*, Vol 4, No. 2, (2018), 402-412. Doi: 10.28991/cej-0309100.
- Bormann, N. E. and Julien, P. Y. Scour Downstream of Grade-Control Structures. *Journal of Hydraulic Engineering*, ASCE, Vol 131, No. 10, (1991), 898-908.
- Jafari, Seyed Reza, and Majid Pasbani Khiavi. “Parametric Study of the Modal Behavior of Concrete Gravity Dam by Using Finite Element Method.” *Civil Engineering Journal*, Vol 5, No. 12 (2019), 2614-2625. doi:10.28991/cej-2019-03091437.
- Mason, P.J. and Arumugan, K., Free jet scour below dams and flip bucket, *Journal of Hydraulic Engineering*, ASCE, Vol. 111, (1985). 220-235. Doi: 10.1061/(asce)0733-9429(1985)111:2(220)
- Amanian, N. and Urroz, G. E.. Design of Pre-excavated Scour Hole Below Flip-bucket Spillways. Proceedings of the 1993 ASCE National Conference on Hydraulic Engineering, San Francisco, (1993), 856-860.
- Stein, O. R., P. Y. Julien, and C. V. Alonso. "Mechanics of jet scour downstream of a headcut." *Journal of Hydraulic Research*, Vol 31, No. 6, (1993), 723-738. Doi: 10.1080/00221689309498814
- Al-Ani, Rami Raad Ahmed, and Basim Hussein Khudair Al-Obaidi. “Prediction of Sediment Accumulation Model for Trunk Sewer Using Multiple Linear Regression and Neural Network Techniques.” *Civil Engineering Journal*, Vol 5, No. 1, (2019), 82. Doi: 10.28991/cej-2019-03091227
- Cordier, Clémence, Killian Guyomard, Christophe Stavrakakis, Patrick Sauvade, Franz Coelho, and Philippe Moulin. “Culture of Microalgae with Ultrafiltered Seawater: A Feasibility Study.” *SciMedicine Journal*, Vol 2, No. 2, (2020), 56-62. doi: 10.28991/scimedj-2020-0202-2..
- Hoffmans, G. J., and H. J. Verheij. "Scour Manual Vol. 96, (1997).
- Khalifehei, Kamran, Gholamreza Azizyan, Mahmood Shafai-Bajestan, and Kwok-wing Chau. "Stability of A-Jack concrete block armors protecting the riverbeds." *Ain Shams Engineering Journal*, (2020). Doi: 10.1016/j.asej.2020.04.018.
- Ghodisian, M., Melville, B., Coleman, S., "Scour caused by rectangular impinging jet in cohesiveless beds", Proc. Third International Conference on scour and erosion, ICSE, Nov. (2006). 1-3, Amsterdam, The Netherlands.
- Juon, R., and W. H. Hager. Flip bucket without and with deflectors. *Journal of Hydraulic Engineering*, Vol 126, No. 11, (2000), 837-845. Doi: 10.1061/(asce)0733-9429(2000)126:11(837).
- Pagliara, Stefano, Willi H. Hager, and Hans-Erwin Minor. "Plunge pool scour in prototype and laboratory." In Proc., Int. Conf. Hydraulics of Dams and River Structures, 165-172. Lisse, the Netherlands: Balkema, 2004. Doi: 10.1201/b16994-24.
- O. A. Yamini, M. R. Kavianpour, and S. Hooman Mousavi. “Wave Run-up and Rundown on ACB Mats Under Granular and Geotextile Filters’ Condition.” *Marine Georesources & Geotechnology* Vol 36, No. 8, (2017), 895-906. doi:10.1080/1064119x.2017.1397068.
- Movahedi, Azin, M. R. Kavianpour, and O. Aminoroayaie Yamini. "Evaluation and modeling scouring and sedimentation around downstream of large dams." *Environmental Earth Sciences*, Vol 77, (2018), 1-17. Doi: 10.1007/s12665-018-7487-2.
- Khatsuria, Rajnikant M. Hydraulics of spillways and energy dissipators. CRC Press, (2004). Doi: 10.1201/9780203996980-24.
- Zhang, S., Pang, B., & Wang, G. A new formula based on computational fluid dynamics for estimating maximum depth of scour by jets from overflow dams. *Journal of Hydroinformatics*, (2014), Vol 16, No. 5, 1210-1226.
- Movahedi, Azin, Mohammadreza Kavianpour, and O. A. Yamini. "Experimental and numerical analysis of the scour profile downstream of flip bucket with change in bed material size." *ISH Journal of Hydraulic Engineering*, (2017), 1-15. Doi: 10.1080/09715010.2017.1398111.
- Aminoroayaie Yamini, O., S. H. Mousavi, and M. R. Kavianpour. “Experimental Investigation of Using Geo-Textile Filter Layer in Articulated Concrete Block Mattress Revetment on Coastal Embankment.” *Journal of Ocean Engineering and Marine Energy*, Vol 5, No. 2, (2019), 119-133. Doi: 10.1007/s40722-019-00133-y
- Gamil, Yaser, Ismail Bakar, and Kemas Ahmed. "Simulation and Development of Instrumental Setup to Be Used for Cement Grouting of Sand Soil." *Emerging Science Journal*, Vol. 1, No. 1, (2017), Doi: 10.28991/esj-2017-01112.
- Schoklitsch, A. “Scour downstream of falling jet.” *Water*, Vol 25, No 24, 341-343, (1932).
- Veronese, A. "Erosion de fond en aval d'une decharge." In IAHR, meeting for hydraulic works, Berlin. 1937.

27. Damle, P.M., Venkatraman, C.P., and Desai, S. C., Evaluation of scour below ski-jump buckets of spillways, CWPRS Golden Jubilee Symposia, London (1966).
28. Chee, S. P., and T. Kung. "Piletas de derrubio autoformadas." In 6th Latin American Congress of the International Association for Hydraulic Research, Bogota, Columbia, Paper D, Vol. 7. 1974.
29. Chee, S. P., and P. V. Padiyar. "The stability of blocks subjected to plunging water jets." JAWRA Journal of the American Water Resources Association 5, No. 3, (1969), 57-63.
30. Wu, C.M. (1973). Scour at Downstream End of Dams in Taiwan. In: International Symposium on River Mechanics, Bangkok, Thailand, Vol. I(A 13), 1-6.
31. Martins, R., 1975. Scouring of rocky riverbeds by free-jet spillways. *Water Power Dam Const.* April (1975).
32. Incyht, L. (1982). —Estudio sobre modelo del aliviadero de la Presa Casa de Piedra, Informe Final. DOH-044-03-82, Ezeiza, Argentina.
33. Azmathullah, H. M. Deo, M. C. Deolalikar, P. B. Neural Networks for Estimation of Scour Downstream of a Ski-Jump Bucket. *Journal of Hydraulic Engineering*, ASCE, Vol 117, No. 5, (2005), 579-594. Doi: 10.1061/(asce)0733-9429(2005)131:10(898)
34. Chanson, H. and Yit-Haw T. "Physical modelling of breaking tidal bores: comparison with prototype data." *Journal of Hydraulic Research*, Vol 53, No. 2, (2015), 264-273. Doi: 10.1080/00221686.2014.989458
35. Theingi, Mya, Kay Thi Tun, and Nwe Nwe Aung. "Preparation, Characterization and Optical Property of LaFeO₃ Nanoparticles via Sol-Gel Combustion Method." *SciMedicine Journal* Vol 1, No. 3, (2019), 151-157, doi: 10.28991/scimedj-2019-0103-5.
36. Jalili, Mehdi, Mohamad Reza Ghasemi, and Ali Reza Pifloush. "Stiffness and Strength of Granular Soils Improved by Biological Treatment Bacteria Microbial Cements." *Emerging Science Journal*, Vol 2, No. 4, (2018), Doi: 10.28991/esj-2018-01146.
37. Lim, S. Y., & Chin, C. O. Scour by circular wall jets with non-uniform sediments. *Advances in hydro-science and engineering*, Vol 1 (Part B), (1993), 1989-1994.
38. Naghikhani, A., Noori, R., Sheikhan, H., Ghiasi, B., Estimation of the dimensions of the scour hole in downstream scour of flip bucket jet with granular computing model, Scientific and Research *Journal of Hydraulic*, Vol. 9, No. 3, (2014), 45-60. Doi: 10.1007/s11269-016-1526-0.
39. Mason, P.J., Effects of air entrainment on plunge pool scour. *Journal of Hydraulic Engineering*, Vol 115, No. 3, (1989) 385-399. Doi: 10.1061/(asce)0733-9429(1989)115:3(385).
40. Sofrelec (1980) "Kandadji Dam, Niger, 3rd Phase Design Report," Society Frangaise d'Etudes et de Realisation d'Equipement Electriques, Paris, France, Feb., 1980.
41. Jaeger, C. (1949). Technische Hydraulik (Technical Hydraulics). Birkhiu-ser, Basel, Switzerland (in German).
42. Yen, Ben Chie, ed. Channel flow resistance: centennial of Manning's formula. Water Resources Publication, 1989.
43. Hartung, W. Die Kolkbildung hinter Uberstromen wehren im Hinblick auf eine beweglich Sturzbettgestaltung. Die Wasser Wirtschaft, Vol. 49, No. 1, (1959) 309-313 (in German).
44. Ervine, D.A., Falvey, H.R., Whithers, W., Pressure fluctuations on Plunge pool floors. *Journal Hydraulic Research*. Vol 35, No. 2, (1997). Doi: 10.1080/00221689709498430
45. Castillo, L., Parametrical analysis of the ultimate scour and mean dynamic pressures at plunge pools. Workshop on Rock Scour due to High Velocity Jets (2002). École Polytechnique Fédérale de Lausanne.
46. Melo, J. F., A. N. Pinheiro, and C. M. Ramos. "Forces on plunge pool slabs: Influence of joints location and width." *Journal of Hydraulic Engineering* 132.1 (2006): 49-60.
47. Federspiel, Matteo Paolo Elia Antonio, E. F. R. Bollaert, and A. J. Schleiss. "Dynamic response of a rock block in a plunge pool due to asymmetrical impact of a high-velocity jet." In Proceedings of the 34th World Congress of the International Association for Hydro-Environment Research and Engineering: 33rd Hydrology and Water Resources Symposium and 10th Conference on Hydraulics in Water Engineering, p. 2404. Engineers Australia, 2011.
48. Castillo, L.G., Carrillo, J.M., Characterization of the dynamic actions and scour estimation downstream of a dam. In: Dam Protections against Overtopping and Accidental Leakage. *CRC Press*, (2015), 231-243. Doi: 10.1201/b18292-26.
49. Fiorotto, V., Barjastehmaleki, S., Caroni, E., Stability analysis of plunge pool linings. *Journal Hydraulic Engineering* Vol. 10 No. 3 (2016) Doi: 10.1061/(ASCE)HY.1943-7900.0001175.
50. Yamini, O. Aminoroayaie, M. R. Kavianpour, and Azin Movahedi. "Pressure distribution on the bed of the compound flip buckets." *The Journal of Computational Multiphase Flows*, Vol 7, No. 3, (2015), 181-194. Doi: 10.1260/1757-482x.7.3.181
51. Yamini, O. A., Kavianpour, M. R., & Mousavi, S. H. Experimental investigation of parameters affecting the stability of articulated concrete block mattress under wave attack. *Applied Ocean Research*, Vol. 64, (2017), 184-202, Doi: 10.1016/j.apor.2017.03.003

Persian Abstract

چکیده

پرتابه های جامی شکل به عنوان سازه مستهلک کننده انرژی در انتهای سرریز سدهای بلند به منظور کاهش هزینه ها در مقایسه با دیگر مستهلک کننده های انرژی به کار می رود. در این مطالعه با استفاده از یک مدل آزمایشگاهی به منظور بررسی حفره آبستگي در ناحیه پایین دست سرریزهای پرتاب کننده های جامی در آزمایشگاه هیدرولیک دانشگاه شهید چمران انجام شده است. هدف اصلی از این تحقیق شناسایی حداکثر عمق آبستگي (d_{sm}) و فاصله حداکثر آن از لیفت سطل (L_{sm}) است که برای نیل به این هدف آزمایش های مختلف در شرایط متفاوت برنامه ریزی شده است. نتایج نشان مطالعه حاضر داد که با افزایش دبی، حداکثر عمق آبستگي و فاصله حفره آبستگي از محل پرتابه دورتر خواهد شد. همچنین، با افزایش عدد فرود ذرات Fg و یا کاهش عمق، میزان آبستگي و حفره ایجاد شده گسترش می یابد. در این مطالعه دو رابطه تجربی برای پیش بینی حداکثر عمق آبستگي و فاصله آن از محل سرریز با استفاده از رگرسیون چند متغیره غیرخطی ایجاد شد و صحت سنجی این رابطه با مطالعه گذشته مورد ارزیابی قرار گرفته است. بر اساس رابطه MARE ارائه شده برای نتایج مطالعه حاضر برابر با $34/2$ درصد است که نشان دهنده دقیق تر بودن رابطه ارائه شده است. نتایج این مطالعه می تواند با دقت بسیار زیادی مشخصات حفره آبستگي در پایین دست سرریزهای سدها بزرگ را برای طراحان پیش بینی نماید.
